molecular pharmaceutics

ARTICLE

pubs.acs.org/molecularpharmaceutics

Mannose-Functionalized "Pathogen-like" Polyanhydride Nanoparticles Target C-Type Lectin Receptors on Dendritic Cells

Brenda Carrillo-Conde,[†] Eun-Ho Song,[‡] Ana Chavez-Santoscoy,[†] Yashdeep Phanse,[§] Amanda E. Ramer-Tait,[§] Nicola L. B. Pohl,[†,‡] Michael J. Wannemuehler,[§] Bryan H. Bellaire,[§] and Balaji Narasimhan*[,†]

[†]Department of Chemical and Biological Engineering, [‡]Department of Chemistry, and [§]Department of Veterinary Microbiology and Preventive Medicine, Iowa State University, Ames, Iowa 50011, United States

Supporting Information

ABSTRACT: Targeting pathogen recognition receptors on dendritic cells (DCs) offers the advantage of triggering specific signaling pathways to induce a tailored and robust immune response. In this work, we describe a novel approach to targeted antigen delivery by decorating the surface of polyanhydride nanoparticles with specific carbohydrates to provide "pathogen-like" properties that ensure nanoparticles engage C-type lectin receptors on DCs. The surface of polyanhydride nanoparticles was functionalized by covalent linkage of dimannose and lactose residues using an amine−carboxylic acid coupling reaction. Coculture of functionalized nanoparticles with bone marrow-derived DCs significantly increased cell surface expression of MHC II, the T cell costimulatory molecules CD86 and CD40, the C-type lectin receptor CIRE and the mannose receptor CD206 over the nonfunctionalized nanoparticles. Both non-functionalized and functionalized nanoparticles were efficiently internalized by DCs, indicating that internalization of functionalized nanoparticles was necessary but not sufficient to activate DCs. Blocking the mannose and CIRE receptors prior to the addition of functionalized nanoparticles to the culture inhibited the increased surface expression of MHC II, CD40 and CD86. Together, these data indicate that engagement of CIRE and the mannose receptor is a key mechanism by which functionalized nanoparticles activate DCs. These studies provide valuable insights into the rational design of targeted nanovaccine platforms to induce robust immune responses and improve vaccine efficacy.

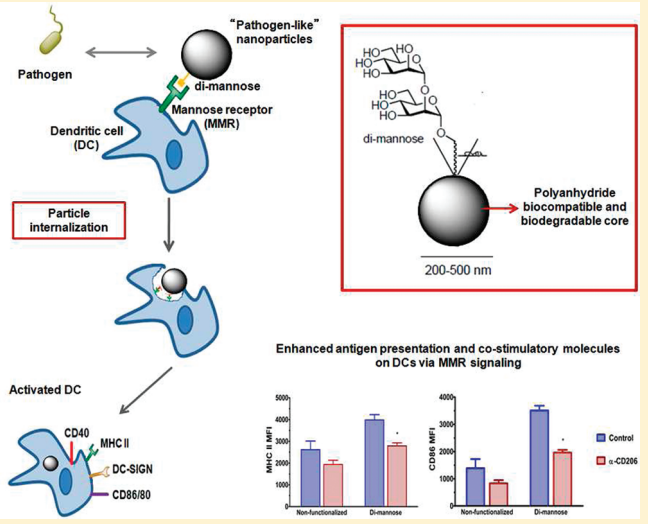

KEYWORDS: polyanhydrides, nanoparticles, carbohydrates, dendritic cells, targeting

INTRODUCTION

The use of vaccine adjuvants to activate the innate immune system is crucial to vaccine effectiveness.[1] Adjuvants can be used to enhance the efficacy of single dose vaccines and reduce the required antigen dose. The use of biodegradable polymer nanoparticles as vaccine delivery vehicles allows for effective delivery of payloads by parental or mucosal administration by protecting the antigen from harsh physiological conditions and enabling transport across biological barriers (e.g., mucus membranes).[2] Polyanhydride nanoparticles have shown excellent potential as vaccine carriers.[3−6] Encapsulation of protein antigens into polyanhydride particles stabilizes them and provides sustained aztnigen release;[4,7] these particles also enhance the immune response by acting as an adjuvant.[3]

Dendritic cells (DCs) are antigen presenting cells (APCs) that play a major role in connecting the innate and adaptive immune systems, a key step to inducing protective immunity.[8] DCs can sense and internalize antigen by a variety of mechanisms that trigger DC maturation and direct further interactions with other immune cells, including naive T cells.[1,9,10] Pattern recognition receptors (PRRs) on DCs detect the presence of a potential threat by interacting with pathogen-associated molecular patterns (PAMPs).[10,11] In particular, C-type lectin receptors (CLRs) are PRRs with highly conserved carbohydrate-recognition domains that bind sugar moieties (e.g., mannose, fucose, and glucan) on the surface of certain pathogens (e.g., *Candida albicans*, *Mycobacterium tuberculosis*, and *Mycobacterium leprae*) in a calcium-dependent manner.[12,13] Ligand recognition by Toll-like receptors, a type of PRR, promotes a cascade of intracellular

Received: April 26, 2011
Accepted: September 1, 2011
Revised: August 26, 2011
Published: September 01, 2011

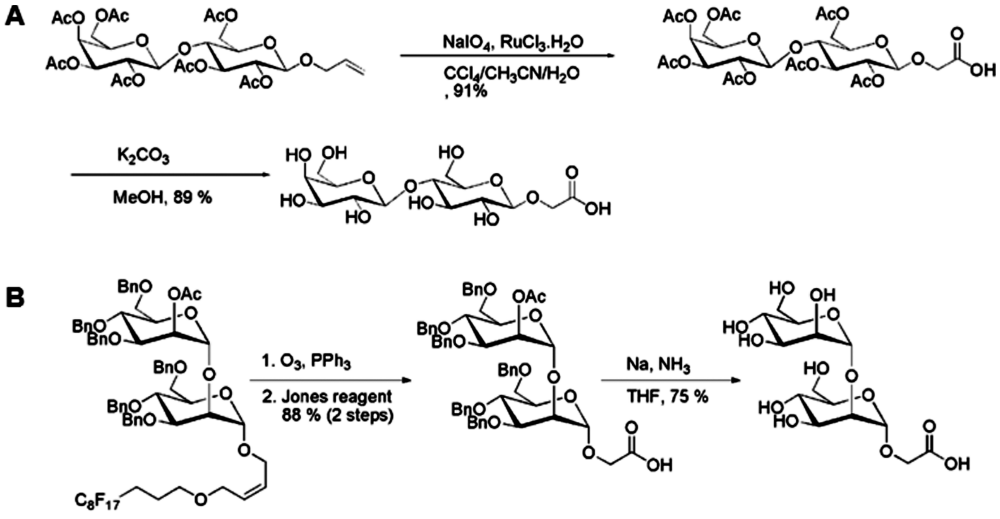

Figure 1. Schematic representation of the synthesis of (A) carboxy-functionalized lactose and (B) carboxy-functionalized dimannose.

signaling events.[14] In addition, ligand recognition by CLRs leads to pathogen internalization via receptor mediated endocytosis and subsequent degradation and presentation of the pathogen as antigen to T cells in the context of MHC I or MHC II, or both.[13,15] Engagement of CLR-associated signaling processes can induce diverse immune responses depending upon the type of carbohydrate ligand bound, the type of responding APC and the engagement of other PRRs on the APC.[12] Thus, the targeting to and the activation of signaling pathways associated with CLRs (e.g., activation of NF-κB signaling pathway) can be a powerful strategy to tailor the immune response.[11,13,14]

Previous studies have demonstrated the potential of targeting CLRs to induce DC maturation and activation; these studies focused on the use of mannoproteins from pathogens[16] or the conjugation of glycans directly to the antigen.[17] Limited studies have explored the use of carbohydrate-functionalized vaccine carriers as targeting vehicles, with most studies using antibodies as ligands.[18] This study outlines a novel approach to target the mannose receptor (CD206) and CIRE (CD209) on murine DCs by mimicking carbohydrate moieties found on the surface of pathogens.[19] Polyanhydride nanoparticle surfaces were functionalized with dimannose in order to study specific interactions with both CLRs known to recognize mannose residues.[10,13] The polyanhydride system used in this study is an amphiphilic copolymer of 1,6-bis(*p*-carboxyphenoxy)hexane (CPH) and 1,8-bis-(*p*-carboxyphenoxy)-3,6-dioxaoctane (CPTEG). The studies described herein demonstrate that mannose-functionalized polyanhydride nanoparticles induce receptor-mediated activation of DCs that may be exploited to enhance the adjuvanticity of this targeted delivery platform.

MATERIALS AND METHODS

Materials. Chemicals needed for monomer synthesis and polymerization, as well as for nanoparticle fabrication, including *p*-carboxybenzoic acid (99+%), and 1-methyl-2-pyrrolidinone, anhydrous (99+%), were purchased from Aldrich (Milwaukee, WI); 4-*p*-hydroxybenzoic acid, 1,6-dibromohexane, 1-methyl-2 pyrrolidinone, and triethylene glycol were purchased from Sigma Aldrich (St. Louis, MO); 4-*p*-fluorobenzonitrile was obtained from Apollo Scientific (Cheshire, U.K.); potassium carbonate, dimethyl formamide, toluene, sulfuric acid, acetic acid, acetonitrile, acetic anhydride, methylene chloride, pentane, and petroleum ether were purchased from Fisher Scientific (Fairlawn, NJ).

Monomer and Polymer Synthesis. CPTEG:CPH copolymers were synthesized by melt polycondensation as described previously.[20] The chemical structure was characterized with ^{1}H NMR, and the molecular mass was determined using gel permeation chromatography (GPC).[20]

Nanoparticle Fabrication. An antisolvent nanoencapsulation method recently published by Ulery et al.[21] was used to fabricate nanoparticles based on a 50:50 molar ratio of CPTEG:CPH copolymers (50:50 CPTEG:CPH). Briefly, polymer was dissolved in methylene chloride (15 mg/mL) held at 4 °C. The polymer solution was rapidly poured into a bath of pentane held at −40 °C at an antisolvent to solvent ratio of 1:150. Particles were collected by filtration and dried under vacuum for 2 h. For fluorescence microscopy studies, FITC−dextran (1% (w/w)) was suspended and homogenized by sonication in the polymer solution prior to precipitation.

Nanoparticle Surface Functionalization. *Synthesis of Carboxylated Lactose and Dimannose.* β-1-*O*-Allylated lactose[22] was prepared through mercury(II)-catalyzed allylation[23] of penta-*O*-acetyl-lactosyl bromide. As expected, use of excess amounts of $NaIO_4$ (8 equiv) under ruthenium-catalyzed Sharpless conditions[24,25] produced the desired acid in 91% yield. Subsequent deacetylation under mild conditions using K_2CO_3 provided the desired fully deprotected disaccharide (Figure 1A).

To obtain the dimannoside, the iterative synthesis of linear α-1,2-linked dimannose with a fluorous allyl group using fluorous-solid phase extraction (FSPE) served as the model.[26−28] Carboxylmethyl- dimannose was obtained by ozonolysis of the alkene,[29] followed by further oxidation with Jones reagent.[26] Global deprotection under Birch reduction[30] furnished the fully deprotected α-1,2-linked dimannose (Figure 1B).

Surface Functionalization. Lactose and dimannose were conjugated on the surface of polyanhydride nanoparticles by an amine−carboxylic acid coupling reaction.[28,30,31] Lactose, a neutral sugar with the same molecular weight as dimannose, was chosen as a control sugar because of its different stereochemical configuration compared to dimannoside. Particles with glycolic

acid groups on the surface (linker groups) and nonfunctionalized (NF) particles were used as controls. An average concentration of 9.6×10^{-4} mmol of COOH/mg of NF nanoparticles was calculated by a theoretical approach using the end groups obtained from ^{1}H NMR spectra and by deconvolution analysis of the C1s high-resolution spectra obtained from X-ray photoelectron spectroscopy (XPS). The conjugation reaction was performed by incubating a nanoparticle suspension (100 mg/mL) with 10 equiv of 1-ethyl-3-(3-dimethylaminopropyl)carbodiimide hydrochloride (EDC), 12 equiv of *N*-hydroxysuccinimide (NHS), and 10 equiv of ethylene diamine in distilled water. This first incubation was carried out at room temperature for 12 h at a constant agitation of 350 rpm. After the incubation period, particles were centrifuged at 10,000 rpm for 10 min and the supernatant was removed. A new incubation was performed with 12 equiv of EDC, 12 equiv of NHS and 10 equiv of the corresponding saccharide (i.e., lactose or dimannose) in distilled water, using constant agitation at 350 rpm for 12 h at room temperature. Particles were sonicated before and after each incubation period to break aggregates. After the reaction was completed, nanoparticles were collected by centrifugation (10,000 rpm, 10 min) and dried under vacuum overnight.

Characterization of Functionalized Nanoparticles. The morphology and size of functionalized and nonfunctionalized nanoparticles were characterized by scanning electron microscopy (SEM, JEOL 840A, JEOL Ltd., Tokyo, Japan) and quasi-elastic light scattering (QELS, Zetasizer Nano, Malvern Instruments Ltd., Worchester, U.K.), respectively. For SEM, samples were vacuum-dried and coated with gold before imaging with the electron microscope. The nanoparticles were suspended in cold water and sonicated for one minute before QELS readings were performed. QELS was also used to determine the ζ-potential of nonfunctionalized and functionalized nanoparticles in order to determine the presence of the disaccharides. XPS (PHI 5500 Multitechnique system, Physical Electronics, Inc., Chanhassen, MN) was used to determine the presence of lactose and dimannose on the surface of polyanhydride nanoparticles. Binding energies were referenced to the aliphatic hydrocarbon peak at 285.0 eV.[32] High-resolution C1s peaks were collected and fitted using CasaXPS software (RBS Instruments, Bend, OR). Finally, a modified and optimized high throughput version of a phenol−sulfuric acid assay[33] was used to quantify the amount of sugar attached to the nanoparticles. The modified assay was performed directly in 96-well plates, and the incubation time was increased to 30 min to allow for equal reduction of the different sugars used to link to the nanoparticles. Nonfunctionalized nanoparticles were used as controls to account for polymer interference with the assay. A microplate reader was used to obtain the absorbance of standards and unknown samples using a wavelength of 490 nm. The total amount of sugar (μg/mg) was calculated by normalization with the nanoparticle mass.

In Vitro DC Uptake and Activation. *Mice.* C57BL/6 (B6) mice were purchased from Harlan Sprague−Dawley (Indianapolis, IN). All mice were housed under specific pathogen-free conditions where all bedding, caging, and feed were sterilized prior to use. All animal procedures were conducted with the approval of the Iowa State University Institutional Animal Care and Use Committee.

DC Culture and Stimulation. Dendritic cells were derived from the bone marrow precursor cells recovered from the femurs and tibias of B6 mice according to a previously published protocol.[34,35] DCs were >90% positive for DC marker CD11c. For flow analysis, nonstimulated (NS) DCs and *Escherichia coli* lipopolysaccharide (LPS) (200 ng/mL) (Sigma Aldrich, St. Louis, MO) treated DCs were used as negative and positive controls, respectively. On day 9 of the culture, nonfunctionalized or functionalized nanoparticles were incubated with DCs for 48 h at a concentration of 0.125 mg/mL, a concentration chosen based on previously published studies.[35] In order to investigate the role of mannose receptor engagement in DC activation by dimannose-functionalized polyanhydride nanoparticles, QJ; DCs were incubated with anti-CD206 (Clone 310301, R&D Systems, Minneapolis, MN) and/or anti-CD209 (Clone LWC06, eBioscience, San Diego, CA) antibodies either individually or in combination at a final concentration of 10 μg/mL for 15 min at room temperature prior to addition of stimulants. Preincubation with anti-CD206 and/or anti-CD209 blocked the cross-linking of the mannose and/or CIRE receptors by sugar-functionalized nanoparticles. This treatment tested the hypothesis that functionalized nanoparticles enhance DC activation via increased mannose and/or CIRE receptor-mediated endocytosis.

Flow Cytometric Analysis. Flow cytometric analysis of surface molecule expression was performed as previously described.[34] Additional antibodies used in this study include FITC anti-mouse CD206 (MMR, clone MR5D3) and the isotype-specific control antibody FITC rat IgG2a κ (clone RTK2748) purchased from BioLegend (San Diego, CA), and biotin anti-mouse CD209 (CIRE, clone 5H10) purchased from eBioscience (San Diego, CA). As noted, the two antibodies used for FACS analysis are different from the antibodies used to block CLRs, thus preventing false negatives due to unavailable binding sites following treatment with the blocking antibody. Samples were acquired on a Becton-Dickinson FACSCanto flow cytometer (San Jose, CA) and the data analyzed using FlowJo (TreeStar Inc., Ashland, OR). Percentage of cells expressing each cell surface marker were obtained by quantifying the peak shift from their respective isotype controls, and the intensity of the expression was reported as mean fluorescence intensity (MFI).

Cytokine Assays. After stimulation for 48 h with nonfunctionalized or functionalized nanoparticles, cell-free supernatants were assayed for IL-1β, IL-10, TNF-α, IL-6, and IL-12p40 using a multiplex cytokine assay in conjunction with a Luminex 100 System (Flowmetrics, Austin, TX) as described elsewhere.[34,35]

Fluorescence Microscopy Analysis of Nanoparticle Uptake by DCs. To visualize nanoparticle interactions with DCs, a previously described experimental protocol for coincubation, immunofluorescence preparation and microscopic observation was followed.[21] In these experiments, an equivalent amount (200 μg/mL) of either nonfunctionalized or functionalized 1% FITC−dextran loaded nanoparticles were incubated with DCs and then washed repeatedly three times with pH 7.4 PBS to remove extracellular and nonadherent particles. DCs coincubated with nanoparticles for 30 min were fixed and analyzed 2 h post uptake. At the indicated times, cultures were fixed for 20 min with 4% paraformaldehyde in pH 7.4 PBS, washed and incubated with 5 μg/mL tetramethylrhodamine-wheat germ agglutinin (WGA) for 10 min at 37 °C. Stained and washed coverslips were mounted on glass slides using Pro-Long w/DAPI mountant (Invitrogen, Carlsbad, CA). Epifluorescence microscopy was performed using an Olympus IX-71 inverted microscope with blue, green, and red filter sets with a cooled CCD camera. Final image preparation and morphometric analysis was performed as described previously utilizing threshholding and particle counting algorithms of ImageJ v1.36b software (NIH, Bethesda, MD).[21]

Table 1. Nanoparticle Characterization[a]

nanoparticle type	average particle diameter (nm)	av particle ζ-potential (mV)	sugar density (μg/mg of particle)
nonfunctionalized	162 ± 43	−20 ± 0.6	
linker	231 ± 52	21 ± 1.5	
lactose	266 ± 44	26 ± 2.4	10.9 ± 6.8
dimannose	278 ± 32	28 ± 3.2	12.4 ± 5.5

[a] Nonfunctionalized and functionalized nanoparticles were characterized by QELS and zeta potential measurements. Particle size data represent the mean value ± standard deviation (SD) of dynamic light scattering data collected in three independent experiments. Zeta potential data represent the mean value ± SD of three independent readings. Change in zeta potential clearly indicates that sugars were efficiently conjugated to the 50:50 CPTEG:CPH nanoparticles' surface. Sugar density on nanoparticles' surface was determined by a colorimetric phenol−sulfuric acid assay. Amount of sugar was determined relative to standard curves; data is presented as mean ± SD of four independent experiments.

Binary data was extracted from grayscale images collected from the FITC bandpass filter set using equivalent exposure settings from fixed samples of DCs various nanoparticle modifications. For each sample, images from 5 fields of view (FOV) were collected and compiled with all grayscale images, including the 5 FOV from the various nanoparticle formulations. The compiled image set was then batch treated for background subtraction and thresholding using parameters set according to negative (no particle) control cultures that were performed in parallel for each experiment and time point. Results presented are compiled from three separate biological replicates.

Statistical Analysis. The statistical software JMP7 was used to analyze the cell surface marker, cytokine, and internalization data. One-way ANOVA and Tukey's HSD were used to determine statistical significance among treatments, and p-values <0.05 were considered significant.

RESULTS

Polymer Synthesis. A 50:50 molar ratio copolymer of CPTEG and CPH was synthesized as previously described.[20] This formulation was chosen for these studies because previous studies have shown that it preserves protein structure and antigenicity in addition to exhibiting adjuvant properties.[4,5,7,34] ^{1}H NMR spectroscopy was used to characterize the polymer structure, and the spectra were consistent with previously published data.[20] The synthesized 50:50 CPTEG:CPH copolymer had a M_w of 8,500 g/mol with a polydispersity index of 1.7. These values are consistent with previous work.[7,20]

Characterization of Functionalized Nanoparticles. Particle morphology and size of both nonfunctionalized and functionalized-nanoparticles were analyzed by SEM (data not shown). Some aggregation was observed after surface functionalization, which was attributed to the reaction conditions. The aggregation was disrupted by sonicating the nanoparticles before use, as indicated by the size distribution profiles of the sonicated nanoparticles obtained by QELS (Table 1). No significant differences were observed between the size of the functionalized and the nonfunctionalized nanoparticles.

Measurements of ζ-potential using QELS were employed to characterize the nanoparticle surface functionalization (Table 1). The nonfunctionalized nanoparticles exhibited a ζ-potential of −20 mV. In contrast, the various functionalized nanoparticles resulted in a positively charged ζ-potential (ranging from 20 to 26 mV). The positive charge observed after functionalization is attributed to the presence of the diamine linker on the surface of the particles; this was corroborated by analyzing the ζ-potential of nanoparticles that were only reacted with the ethylene diamine linker but without glycolic acid or sugar. This control showed a slightly more positive ζ-potential in comparison to the linker and sugar modified particles. As expected, the reaction yield of sugar attachment to the linker is not 100%. Since the dimannoside is a neutral sugar, the free amine groups present on the surface of the particles are responsible for the positive charge observed.

Table 2. X-ray Photoelectron Spectroscopy (XPS) Analysis of Atomic Percentages and Ratios of Elements Present on Nonfunctionalized and Functionalized 50:50 CPTEG:CPH Nanoparticles[a]

nanoparticle type	% C[b]	% N[b]	% O[b]	O/C[c]	N/C[c]
nonfunctionalized	74.9 ± 1.5	1.2 ± 0.1	23.9 ± 2.3	0.320	0.016
linker	65.5 ± 0.9	4.4 ± 0.5	18.1 ± 1.9	0.276	0.067
lactose	76.3 ± 2.1	5.1 ± 0.4	20.9 ± 1.1	0.274	0.067
dimannose	73.9 ± 1.1	5.3 ± 0.7	23.3 ± 1.5	0.315	0.072

[a] An increase in the nitrogen content of functionalized nanoparticles correlates with the presence of the amine linker used in the amine−carboxylic acid reaction. [b] Data reported as mean ± standard deviation of four independent experiments performed in triplicate. [c] Ratio of the two elements as indicated.

The functionalized nanoparticles were characterized using XPS[36] to quantitatively determine successful linker and sugar conjugation to the nanoparticle surface. Table 2 shows the surface elemental atomic percentages and elemental ratios of nonfunctionalized and functionalized nanoparticles. Clear differences in the N/C ratio were observed, showing a significant increase in nitrogen content (i.e., 0.01 in the nonfunctionalized particles to almost 0.07 in the functionalized particles). This increase in nitrogen content is directly related to the presence of the amine linker. The presence of nitrogen groups on the surface makes the surface composition of these particles similar to that of pathogens, which are known to have a high content of amine-containing compounds.[37]

High-resolution C1s spectra were fitted with four main components according to their characteristic binding energies representing aliphatic hydrocarbon at 285.0 eV (C1), ether and amine groups at 286.5 eV (C2), carbonyl and amide groups at 288.2 eV (C3), and ester and carboxylic acid groups at 289.1 eV (C4).[32] Analysis of C1s spectra allows for more direct comparison of sugar attachment based on increases in the ether and amine groups (C2). Ether groups are characteristic of carbohydrate structures while the amine groups are indicative of the presence of the amine linker used for surface modification. Table 3 shows the average percentage areas obtained from high-resolution C1s fitted spectra. These data indicate a clear increase in the C2 component in the functionalized-nanoparticle groups, especially those functionalized with lactose and dimannose. The C2 component percentage for the nonfunctionalized 50:50 CPTEG:CPH nanoparticles is ∼22%, while that of the sugar-functionalized nanoparticles is ∼30%. It is known that the outer surface of bacterial pathogens is composed of various constituents bearing amine and hydroxyl groups (e.g., peptidoglycan, lipopolysaccharide, lipoproteins, and flagella).[37] Analysis of C1s (Table 3) and

Table 3. Average Percentage Areas of Aliphatic Hydrocarbon (C1), Ether and Amine Groups (C2), Carbonyl and Amide Groups (C3), and Ester and Carboxylic Acid Groups (C4)[a]

	percentage area of C1s components[b]			
nanoparticle type	C1	C2	C3	C4
nonfunctionalized	59.7 ± 1.2	22.3 ± 0.7	8.7 ± 0.6	1.4 ± 0.1
linker	58.3 ± 1.7	26.6 ± 0.7	7.1 ± 0.3	0.1 ± 0.2
lactose	58.2 ± 0.8	30.1 ± 1.2	6.6 ± 0.6	0.6 ± 0.1
dimannose	58.1 ± 1.9	29.6 ± 1.0	6.9 ± 0.5	0.4 ± 0.1

[a] Obtained from XPS high-resolution C1s fitted spectra. Increased surface presence of ether, amine and hydroxyl groups corroborated nanoparticle functionalization. [b] Data reported as mean ± standard deviation of four independent experiments performed in triplicate.

O1s (data not shown) spectra of functionalized nanoparticles showed a clear increase of amine, ether, and hydroxyl groups, resulting in a surface composition that is similar to that of pathogens.[37] The total amount of sugar attached to the nanoparticle surface was quantified by the phenol−sulfuric acid assay. The results showed that similar amounts (12.6 ± 6.4 μg/mg of particle) of lactose and dimannose were attached to the 50:50 CPTEG:CPH nanoparticles (Table 1).

Dimannose-Functionalized Nanoparticles Enhanced DC Expression of MHC II, Costimulatory Molecules and CLRs. Flow cytometry was used to determine if functionalized nanoparticles enhanced the activation status of DCs. In general, the results indicate that dimannose-functionalized nanoparticles significantly enhanced the expression of key surface markers that are associated with DC maturation and antigen presentation (i.e., MHC II, CD86, and CD40) and concomitantly increased the surface expression of CLRs (i.e., CD206 and CIRE) as compared to nonfunctionalized nanoparticles (Figure 2). Another interesting observation from these studies is that the dimannose-functionalized nanoparticles induced higher expression of both CD206 and CIRE as compared to lactose-functionalized particles, confirming the specificity of both CIRE and CD206 for mannose residues as observed previously.[13]

Soluble lactose and dimannose and nonfunctionalized nanoparticles plus soluble sugar were used as controls to probe the benefit of the covalent linkage of the sugars to the nanoparticle surface. The addition of soluble sugars (i.e., lactose and dimannose) to cultures of DCs with nonfunctionalized nanoparticles did not significantly change cell surface marker expression from levels induced by the nonfunctionalized nanoparticles alone (Supplemental Figure 1 in the Supporting Information).

Stimulation with Functionalized Nanoparticles Enhanced Proinflammatory Cytokine Secretion. Although stimulation of DCs with either nonfunctionalized or functionalized nanoparticles modestly increased the secretion of IL-6 in comparison to the nonstimulated controls, the greatest amounts of IL-6 were produced by DCs stimulated with linker-modified nanoparticles (black bars in Figure 3). Elevated levels of TNF-α were secreted (gray bars in Figure 3) upon stimulation with the linker-functionalized particles. Neither IL-10 nor IL-1β was detected in the culture supernatants (data not shown). This observation is consistent with previously published work with other polyanhydride chemistries[35] and different particle sizes.[34] The level of IL-12p40 secreted into the culture medium by DCs stimulated with either nonfunctionalized or functionalized nanoparticles was not statistically different from the nonstimulated controls (data not shown).

Both Nonfunctionalized and Functionalized Nanoparticles Were Efficiently Internalized by DCs. Microscopic analyses were performed to determine if the enhanced activation of DCs by functionalized nanoparticles was associated with enhanced internalization. Interestingly, all the functionalized nanoparticle groups were efficiently internalized following 30 min of coincubation with DCs (Figure 4A). These qualitative findings were corroborated by morphometric analysis of the epifluorescent images of the FITC-loaded nanoparticles, which is presented as the total area (μm^2) of internalized nanoparticles. This metric allowed us to perform biologically relavent comparisons among all treatments. The morphometric analysis revealed that higher amounts of functionalized nanoparticles were internalized by DCs when compared to nonfunctionalized nanoparticles (Figure 4B).

Mannose Receptor-Mediated Activation of DCs by Dimannose-Functionalized Nanoparticles. To test the specificity of the dimannose functionalization for binding to CLRs, monoclonal antibodies were used to inhibit activation of the mannose receptor and CIRE on DCs stimulated with nonfunctionalized and dimannose-functionalized nanoparticles (Figure 5). For all the surface markers evaluated (i.e., MHC II, CD40, CD86, CD209, and CD206), the mean fluorescence intensity (MFI) values for the nonstimulated DCs did not change over that of the controls when the monoclonal antibodies against the CLRs were added, indicating that no additional stimulation was provided by the antibodies used as blocking agents. After blocking with anti-CD209 or anti-CD206, a reduction in the expression of CIRE and CD206, respectively, was observed after stimulation with dimannose-functionalized nanoparticles (as shown in Figure 5D and 5E). This result demonstrates that the use of specific monoclonal antibodies can block the upregulation of the mannose and CIRE receptors induced by dimannose-functionalized particles. Furthermore, when the anti-CD206 monoclonal antibody was used, the increased surface expression of MHC II, CD40, and CD86 was inhibited (Figures 5A, 5B and 5C). This outcome demonstrates that mannose receptor engagement by the functionalized nanoparticles plays a critical role in their adjuvant effect. In these experiments, the linker and lactose-functionalized particles were also added to separate DC cultures to control for the specificity of the blocking antibodies. After pretreatment with the anti-CD206 monoclonal antibody, there was no significant inhibition in the expression of MHC II, CD40, and CD86 (Supplemental Figure 2 in the Supporting Information), further corroborating the specificity of the mannose receptor mediating DC activation by the dimannose-functionalized nanoparticles.

DISCUSSION

Engineering nanoparticles that are targeted to specific receptors on APCs offers a novel approach for the rational design of effective vaccine adjuvants. The covalent linkage of specific carbohydrates to the surface of nanoparticles allows for the targeting of CLRs and activation of complex signaling pathways including crosstalk with other PRRs (e.g., TLRs and Fc receptors) that can direct the immune response. The data presented herein demonstrate the design and fabrication of novel dimannose-functionalized polyanhydride nanoparticles that possess characteristically similar chemical compositions as that of pathogen surfaces. These "pathogen-like" nanoparticles were efficiently

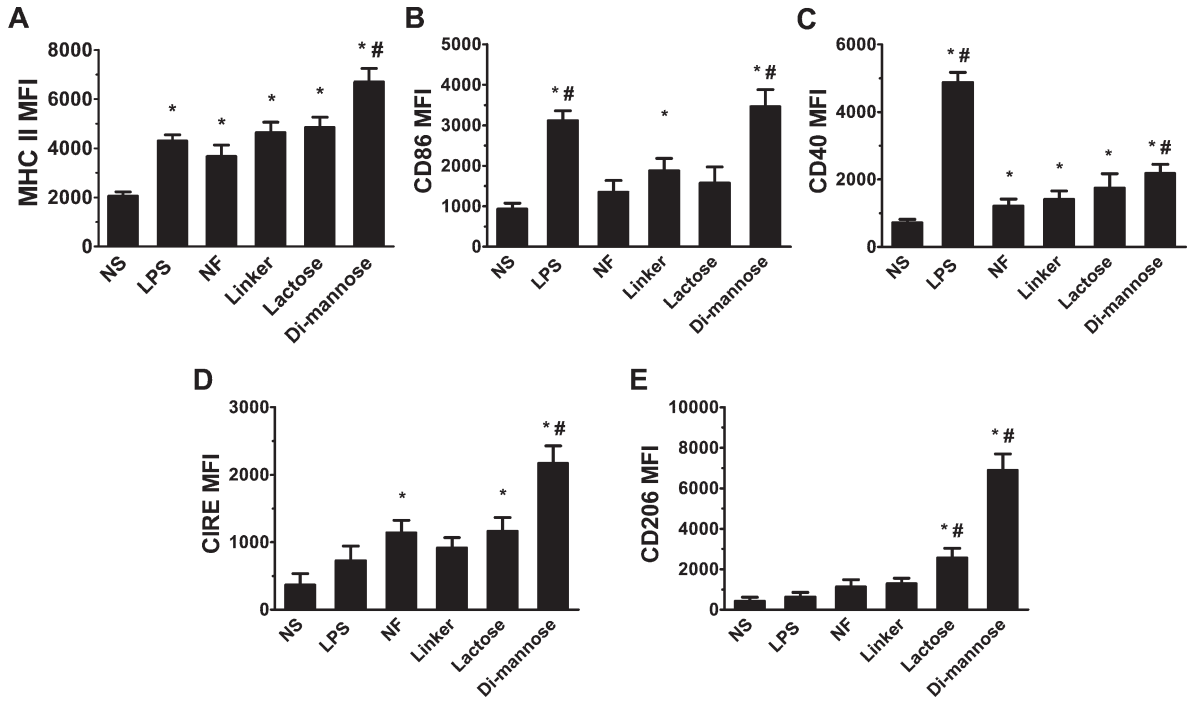

Figure 2. Dimannose-functionalized nanoparticles enhanced DC expression of MHC II, costimulatory molecules and C-type lectin receptors (CLRs). After stimulation with either nonfunctionalized (NF) or functionalized nanoparticles for 48 h, DCs were harvested and analyzed by flow cytometry for surface expression of (A) MHC II, (B) CD86, (C) CD40, (D) CIRE, or (E) CD206. LPS stimulated and nonstimulated cells (NS) were used as positive and negative controls, respectively. Data are expressed as the mean ± the SEM of four independent experiments performed in triplicate. * and # represent groups that are statistically significant ($p \leq 0.05$) compared to the NS or NF groups, respectively. MFI = mean fluorescence intensity.

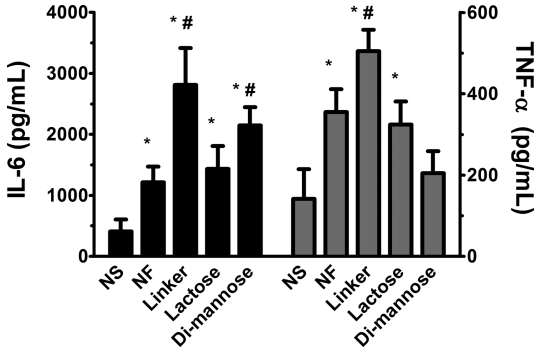

Figure 3. Stimulation with functionalized nanoparticles enhanced secretion of proinflammatory cytokines from DCs. After stimulation with nonfunctionalized (NF) or functionalized nanoparticles for 48 h, supernatants were harvested and assayed for IL-6 (black bars) and TNF-α (gray bars). Data is represented as mean concentration of cytokines ± the SEM of four independent experiments performed in triplicate. LPS was used as a positive control stimulant (>50,000 pg/mL for IL-6 and 6,861 pg/mL for TNF-α), and nonstimulated cells (NS) were used as a negative control. * and # represent groups that are statistically significant ($p \leq 0.05$) compared to the NS or NF groups, respectively.

internalized by DCs (Figure 4) and concomitantly activated DCs (Figures 2 and 3) *in vitro* by specific interactions with the mannose receptor (Figure 5).

All the particles (i.e., nonfunctionalized and linker, lactose, and dimannose-functionalized) enhanced the expression of MHC II, CD40, and CIRE (Figures 2A, 2C and 2D) when compared to nonstimulated DCs. While nonfunctionalized 50:50 CPTEG: CPH nanoparticles demonstrated moderate DC activation, dimannose functionalization of the nanoparticles induced greater expression of MHC II, CD40, and CD86. MHC II, CD40, and CD86 play an important role in the induction of adaptive immunity through activation of $CD4^+$ T cells, and it would be beneficial for an effective adjuvant to enhance the expression of MHC II and costimulatory molecules.[1,9,34]

CIRE and the mannose receptor play an important role in antigen uptake, as well as in DC migration and initial interaction with T cells.[9−11,13] As mentioned before, the activation of CLR-induced signaling processes can result in the induction of diverse immune responses.[12] As shown in Figures 5D and 5E, by chemically conjugating dimannose to the surface of polyanhydride nanoparticles, effective cross-linking of CLRs on DCs was achieved, resulting not only in a higher expression of both CIRE and CD206 but also in higher expression of other DC maturation markers (i.e., MHC II, CD40, and CD86) compared to the nonfunctionalized particles. High affinity binding of CLRs to their ligands is known to result in increased expression of the receptor on the cell surface.[38] Additionally, the results presented in Supplemental Figure 1 in the Supporting Information demonstrate that the sugars must be covalently attached to the nanoparticles to enhance the activation of the DCs. Finally, the data presented in Supplemental Figure 2 in the Supporting Information further corroborates the binding of the dimannose-functionalized nanoparticles to the mannose receptor in order to enhance the activation of DCs.

The expression of MHC II, CD86 and CD40 is essential for antigen presentation and activation of naive T cells; however, it is not sufficient to induce an effective T cell response. In the context of a robust immune response, DCs need to secrete an appropriate profile of cytokines to enhance $CD4^+$ T cell activation. The data

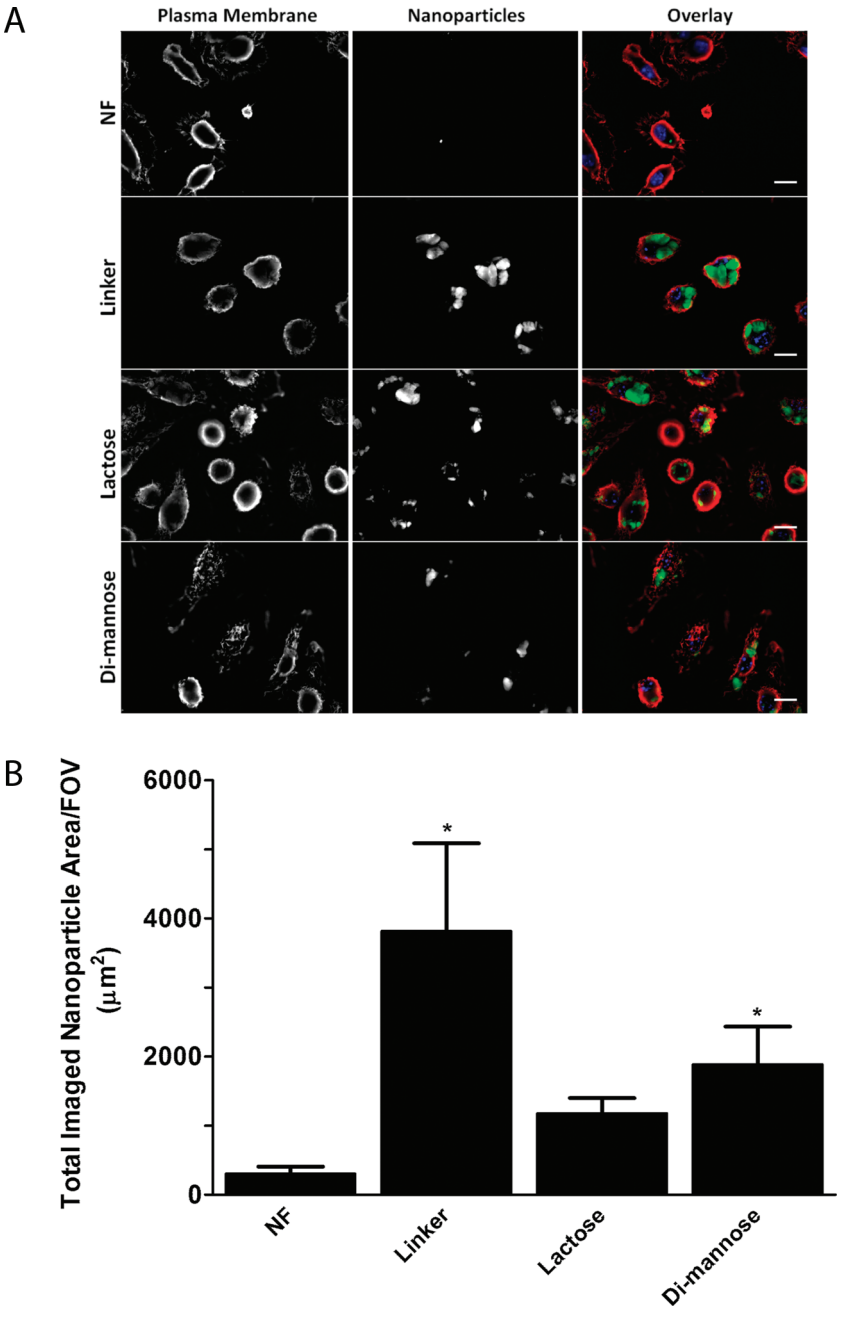

Figure 4. Both nonfunctionalized and functionalized nanoparticles (green) were efficiently internalized by DCs after coincubation for 30 min. Monolayers incubated for 2 h postinternalization with FITC-loaded nanoparticles were stained with WGA conjugated with tetramethylrhodamine to delineate the plasma membrane. (A) Epifluorescent microscopy demonstrated that nanoparticle functionalization enhanced internalization when compared to nonfunctionalized (NF) nanoparticles. Representative epifluorescent images were captured using identical exposure conditions. (B) Quantitative morphometric analysis measuring nanoparticle uptake per field of view (FOV). Data is reported as the total area of fluorescence detected within each FOV (* represents groups that are statistically significant ($p \leq 0.05$) compared to the NF group). Images shown are representative of four fields of view analyzed for each group and consistently observed over three independent experiments. Scale bar = 20 μm.

presented in Figure 3 demonstrate that DCs secreted IL-6 after stimulation with both nonfunctionalized and functionalized nanoparticles. IL-6 is important to both innate and adaptive immune response, as it contributes to systemic inflammation[1] and promotes humoral immune responses.[39] Linker-functionalized nanoparticles also induced the secretion of TNF-α. This cytokine is important in early DC maturation and further induction of T cell differentiation, and, therefore, even small amounts can influence the bias and magnitude of an immune response. Production of these two cytokines by DCs has been previously associated with CLR-induced signaling events.[12,16]

The observed enhancement in surface molecule expression (Figure 2) and IL-6 secretion (Figure 3) by DCs after stimulation with dimannose-functionalized nanoparticles was hypothesized to be related to an increase in particle internalization.[40] However, as shown in Figure 4, all functionalized nanoparticles were efficiently internalized by DCs. In particular, both linker and dimannose-functionalized nanoparticles were present in higher

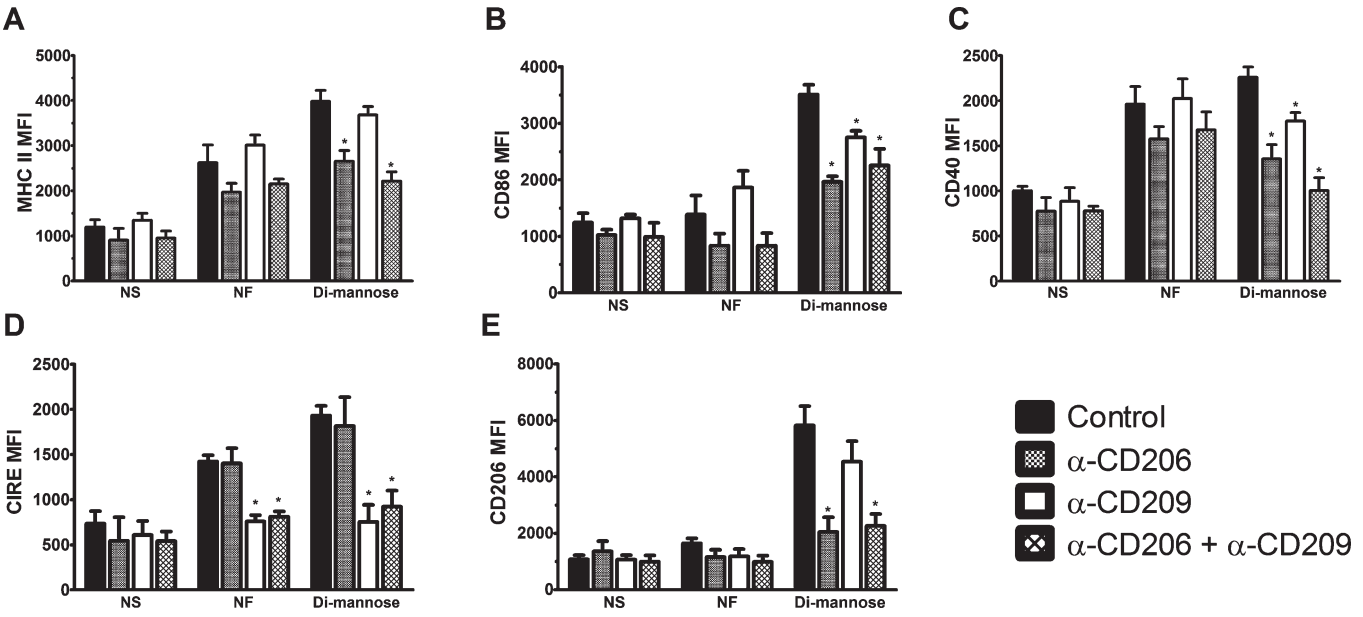

Figure 5. Mannose receptor-mediated activation of DCs by dimannose-functionalized nanoparticles is inhibited by receptor-specific monoclonal antibodies. DC cultures were incubated for 15 min with either α-CD206, α-CD209 or α-CD206 + α-CD209, or medium (control, NS) and then were stimulated with either nonfunctionalized (NF) or dimannose-functionalized nanoparticles for 48 h. DCs were harvested and analyzed via flow cytometry for changes in surface expression of (A) MHC II, (B) CD86, (C) CD40, (D) CIRE, or (E) CD206. MFI (mean fluorescence intensity) $\pm$ the SEM of each of the markers of two independent experiments performed in triplicate is presented. * represents groups that are statistically significant ($p \leq 0.05$) compared to the control treatment.

numbers inside the DCs than nonfunctionalized and lactose-functionalized nanoparticles. These data indicate that particle internalization is *necessary* but not *sufficient* for enhanced DC activation. Previous work from our laboratories has demonstrated enhanced internalization of soluble antigen by monocytes when delivered with nonfunctionalized polyanhydride nanoparticles.[21] Therefore, the results presented in Figure 4 suggest that the functionalized nanoparticles would also provide efficient antigen delivery.

The specific interaction of functionalized nanoparticles with CLRs documented in this study presents an intriguing opportunity for the rational design of nanovaccines possessing the capacity to induce diverse immune responses tailored for a target disease. While the increased activation of DCs with dimannose-functionalized particles was directly correlated with a receptor–ligand interaction, the enhanced internalization of linker-functionalized nanoparticles represents a nonspecific interaction that may be dictated by the positive charge of the functionalized particles. It is well-known that cationic particles show greater adhesion with cell membranes[41] and, therefore, may be an explanation for the enhanced cellular uptake of the linker-functionalized nanoparticles observed in this study. In addition, the nonspecific interaction due to the linker-functionalized nanoparticles may closely mimic the interaction between DCs and endogenous danger signals. Indeed, cellular recognition of endogenous (e.g., hyaluronic acid, uric acid crystals) and exogenous (e.g., LPS, lipoteichoic acid) hydrophobic moieties is an important component of the danger hypothesis describing activation of innate immune responses.[42,43] Nonfunctionalized polyanhydride nanoparticles present a hydrophobic surface to DCs in much the same manner as would apoptotic cells or endogenous stressors compared to the more robust responses induced by microbial PAMPs. Endogenous danger signals are known to stimulate a robust adaptive immune response in the absence of deleterious inflammatory responses,[42] an attribute that would be valuable to replicate when developing safe and effective vaccines. Collectively, these results indicate that polyanhydride nanoparticles can be rationally functionalized to effectively enhance activation of APCs and lead to the design of efficacious targeted vaccine delivery platforms.

CONCLUSIONS

In this study, novel "pathogen-like" particles were fabricated by functionalizing the surface of polyanhydride nanoparticles with sugar residues. The ability of these novel particles to induce and enhance DC activation by specific interactions with the mannose receptor was demonstrated. Targeting CLRs on DCs with ligands covalently linked to polyanhydride nanoparticles has the potential to efficiently deliver antigens to DCs for effective processing and presentation to T cells. A specific ligand–receptor interaction (i.e., dimannose–CD206) was identified by blocking the mannose receptor on DCs, which resulted in the inhibition of DC activation. This data indicates that mannose receptor signaling pathways are involved in the expression of surface molecules required for antigen presentation and T cell costimulation. The receptor-mediated endocytosis induced by the direct interaction of mannose residues with the mannose receptor may be exploited to design efficacious nanovaccines. The initial interactions of these novel dimannose-functionalized nanoparticles with CLRs on DCs have been demonstrated in these studies; however, the biological consequences of these interactions still need to be evaluated and are a continued area of investigation in our laboratories.

ASSOCIATED CONTENT

Supporting Information. Supplemental data on the effect of adding soluble sugars to cultures of DCs with nonfunctionalized

nanoparticles and the effect of adding linker- and lactose-functionalized nanoparticles to the cells that were treated with the blocking antibodies. This material is available free of charge via the Internet at http://pubs.acs.org.

AUTHOR INFORMATION

Corresponding Author

*Iowa State University, Department of Chemical and Biological Engineering, 2035 Sweeney Hall, Ames, Iowa 50011, United States. E-mail: nbalaji@iastate.edu. Phone: (515) 294-8019. Fax: (515) 294-9273.

ACKNOWLEDGMENT

The authors would like to acknowledge financial support from the ONR-MURI Award (NN00014-06-1-1176). This material is based upon work supported by the National Science Foundation under Grant No. EEC 0851519. The authors would also like to thank Shawn Rigby for his expertise in flow cytometry and James Anderegg of Ames Laboratory for his expertise in XPS.

REFERENCES

(1) Wilson-Welder, J. H.; Torres, M. P.; Kipper, M. J.; Mallapragada, S. K.; Wannemuehler, M. J.; Narasimhan, B. Vaccine adjuvants: current challenges and future approaches. *J. Pharm. Sci.* **2009**, *98* (4), 1278–316.

(2) Yuki, Y.; Kiyono, H. Mucosal vaccines: novel advances in technology and delivery. *Expert Rev. Vaccines* **2009**, *8*, 1083–97.

(3) Kipper, M. J.; Wilson, J. H.; Wannemuehler, M. J.; Narasimhan, B. Single dose vaccine based on biodegradable polyanhydride microspheres can modulate immune response mechanism. *J. Biomed. Mater. Res., Part A* **2006**, *76*, 798–810.

(4) Lopac, S. K.; Torres, M. P.; Wilson-Welder, J. H.; Wannemuehler, M. J.; Narasimhan, B. Effect of polymer chemistry and fabrication method on protein release and stability from polyanhydride microspheres. *J. Biomed. Mater. Res., Part B* **2009**, *91* (2), 938–47.

(5) Torres, M. P.; Determan, A. S.; Anderson, G. L.; Mallapragada, S. K.; Narasimhan, B. Amphiphilic polyanhydrides for protein stabilization and release. *Biomaterials* **2006**, *28*, 108–16.

(6) Tamayo, I.; Irache, J. M.; Mansilla, C.; Ochoa-Repáraz, J.; Lasarte, J. J.; Gamazo, C. Poly(Anhydride) Nanoparticles Act as Active Th1 Adjuvants through Toll-Like Receptor Exploitation. *Clin. Vaccine Immunol.* **2010**, *17* (9), 1356–1362.

(7) Carrillo-Conde, B.; Schiltz, E.; Torres, M. P.; Yu, J.; Phillips, G.; Minion, C.; Wannemuehler, M. J.; Narasimhan, B. Amphipilic polyanhydrides for stabilization of *Yersinia pestis* antigens. *Acta Biomater.* **2010**, *6*, 3110–19.

(8) Banchereau, J.; Steinman, R. M. Dendritic cells and the control of immunity. *Nature* **1998**, *392*, 245–52.

(9) Reddy, S. T.; Swartz, M. A.; Hubbell, J. A. Targeting dendritic cells with biomaterials: developing the next generation of vaccines. *Trends Immunol.* **2006**, *27* (12), 573–80.

(10) Pashine, A.; Valiante, N. M.; Ulmer, J. B. Targeting the innate immune response with improved vaccine adjuvants. *Nat. Med.* **2005**, *11* (4), S63–8.

(11) Foged, C.; Sundblad, A.; Hovgaard, L. Targeting vaccines to dendritic cells. *Pharm. Res.* **2002**, *19* (3), 229–38.

(12) Geijtenbeek, T. B. H.; Gringhuis, S. I. Signalling through C-type lectin receptors: shaping immune responses. *Nat. Rev. Immunol.* **2009**, *9*, 465–80.

(13) Figdor, C. G.; van Kooyk, Y.; Adema, G. J. C-type lectin receptors on dendritic cells and Langerhans cells. *Nat. Rev. Immunol.* **2002**, *21*, 77–86.

(14) Tacken, P. J.; de Vries, I. J. M.; Torensma, R.; Figdor, C. G. Dendritic-cell immunotherapy: from ex vivo loading to in vivo targeting. *Nature* **2007**, *7*, 790–802.

(15) van Kooyk, Y.; Rabinovich, G. A. Protein-glycan interactions in the control of innate and adaptive immune responses. *Nat. Immunol.* **2008**, *9*, 593–601.

(16) Pietrella, D.; Corbucci, C.; Perito, S.; Bistoni, G.; Vecchiarelli, A. Mannoproteins from *Cryptococcus neoformans* promote dendritic cell maturation and activation. *Infect. Immun.* **2005**, *73* (2), 820–7.

(17) Adams, E. W.; Ratner, D. M.; Seeberger, P. H.; Hacohen, N. Carbohydrate-mediated targeting of antigen to dendritic cells leads to enhanced presentation of antigen to T cells. *ChemBioChem* **2008**, *9* (2), 294–303.

(18) Cruz, L. J.; Tacken, P. J.; Bonetto, F.; Buschow, S. I.; Croes, H. J.; Wijers, M.; de Vries, I. J.; Figdor, C. G. Multimodal imaging of nanovaccine carriers targeted to human dendritic cells. *Mol. Pharmaceutics* **2011**, *8*, 520–31.

(19) Fernández, N.; Alonso, S.; Valera, I.; González Vigo, A.; Renedo, M.; Barbolla, L.; et al. Mannose-containing molecular patterns are strong inducers of cyclooxygenase-2 expression and prostaglandin E2 production in human macrophages. *J. Immunol.* **2005**, *174*, 8154–62.

(20) Torres, M. P.; Vogel, B. M.; Narasimhan, B.; Mallapragada, S. K. Synthesis and characterization of novel polyanhydrides with tailored erosion mechanisms. *J. Biomed. Mater. Res., Part A* **2005**, *76A* (1), 102–10.

(21) Ulery, B. D.; Phanse, Y.; Sinha, A.; Wannemuehler, M. J.; Narasimhan, B.; Bellaire, B. H. Polymer chemistry influences monocytic uptake of polyanhydride nanospheres. *Pharm. Res.* **2009**, *26* (3), 683–90.

(22) Mereyala, H. B.; Gurrala, S. R. A highly diastereoselective, practical synthesis of allyl, propargyl 2,3,4,6-tetra-O-acetyl-β-D-gluco, β-D-galactopyranosides and allyl, propargyl heptaacetyl-β-D-lactosides. *Carbohydr. Res.* **1998**, *307* (3−4), 351–54.

(23) Chernyak, A. Y.; Antonov, K. V.; Kochetkov, N. K.; Padyukov, L. N.; Tsvetkova, N. V. Two synthetic antigens related to *Streptococcus pneumoniae* type 3 capsular polysaccharide. *Carbohydr. Res.* **1985**, *141* (2), 199–212.

(24) Carlsen, P. H. J.; Katsuki, T.; Martin, V. S.; Sharpless, K. B. A greatly improved procedure for ruthenium tetroxide catalyzed oxidations of organic compounds. *J. Org. Chem.* **1981**, *46* (19), 3936–38.

(25) Ghosh, M.; Dulina, R. G.; Kakarla, R.; Sofia, M. J. Efficient synthesis of a stereochemically defined carbohydrate scaffold: carboxymethyl 2-acetamido-6-azido-4-O-benzyl-2-deoxy-alpha-D-glucopyranoside. *J. Org. Chem.* **2000**, *65* (24), 8387–90.

(26) Schmidt, R. R.; Jung, K.-H. Trichloroacetimidates. In *Carbohydrates in chemistry and biology,part I: chemistry of saccharides*; Ernst, B., Hart, G. W., Sinaý, P., Eds.; Wiley-VCH: Weinheim, 2000; pp 5−59.

(27) Jaipuri, F. A.; Pohl, N. L. B. Toward solution-phase automated iterative synthesis: fluorous-tag assisted solution-phase synthesis of linear and branched mannose oligomers. *Org. Biomol. Chem.* **2008**, *6*, 2686–91.

(28) Song, E.-H.; Osanya, A. O.; Petersen, C. A.; Pohl, N. L. B. Synthesis of multivalent tuberculosis and *Leishmania*-associated capping carbohydrates reveals structure-dependent responses allowing immune evasion. *J. Am. Chem. Soc.* **2010**, *132* (33), 11428–30.

(29) Park, W. K. C.; Auer, M.; Jaksche, H.; Wong, C.-H. Rapid combinatorial synthesis of aminoglycoside antibiotic mimetics: use of a polyethylene glycol-linked amine and a neamine-derived aldehyde in multiple component condensation as a strategy for the discovery of new inhibitors of the HIV RNA rev responsive element. *J. Am. Chem. Soc.* **1996**, *118*, 10150–55.

(30) Sheehan, J.; Cruickshank, P.; Boshart, G. A convenient synthesis of water-soluble carbodiimides. *J. Org. Chem.* **1961**, *26*, 2525–28.

(31) Staros, J. V.; Wright, R. W.; Swingle, D. M. Enhancement by N-hydroxysulfosuccinimide of water-soluble carbodiimide-mediated coupling reactions. *Anal. Biochem.* **1986**, *156*, 220–2.

(32) Carrillo-Conde, B.; Garza, A.; Andergg, J.; Narasimhan, B. Protein adsorption on biodegradable polyanhydride microspheres. *J. Biomed. Mater. Res., Part A* **2010**, *95A* (1), 40–8.

(33) Masuko, T.; Minami, A.; Majima, T.; Nishimura, S.-I. Carbohydrate analysis by a phenol-sulfuric acid method in microplate format. *Anal. Biochem.* **2005**, *339* (1), 69–72.

(34) Torres, M. P.; Wilson-Welder, J. H.; Lopac, S. K.; Phanse, Y.; Carrillo-Conde, B.; Ramer-Tait, A. E.; et al. Polyanhydride microparticles enhance dendritic cell antigen presentation and activation. *Acta Biomater.* **2011**, *7* (7), 2857–64.

(35) Petersen, L. K.; Xue, L.; Wannemuehler, M. J.; Rajan, K.; Narasimhan, B. The simultaneous effect of polymer chemistry and device geometry on the in vitro activation of murine dendritic cells. *Biomaterials* **2009**, *30*, 5131–42.

(36) Colea, M. A.; Thissenb, H.; Losica, D.; Voelcker, N. H. A new approach to the immobilisation of poly(ethylene oxide) for the reduction of non-specific protein adsorption on conductive substrates. *Surf. Sci.* **2007**, *601* (7), 1716–25.

(37) Moat, A. G.; Foster, J. W.; Spector, M. P. *Microbial Physiology*; Wiley-Liss, Inc.: New York, NY; 2002; 715 pp.

(38) Su, S. V.; Gurney, K. B.; Lee, B. Sugar and spice: viral envelope-DC-SIGN interactions in HIV pathogenesis. *Curr. HIV Res* **2003**, *1*, 87–99.

(39) Rincon, M.; Anguita, J.; Nakamura, T.; Fikrig, E.; Flavell, R. A. Interleukin (IL)-6 directs the differentiation of IL-4-producing $CD4^+$ T cells. *J. Exp. Med.* **1997**, *185*, 461–9.

(40) Wijagkanalan, W.; Kawakami, S.; Takenaga, M.; Igarashi, R.; Yamashita, F.; Hashida, M. Efficient targeting to alveolar macrophages by intratracheal administration of mannosylated liposomes in rats. *J. Contr. Rel.* **2008**, *125* (2), 121–30.

(41) Vasir, J. K.; Labhasetwar, V. Quantification of the force of nanoparticle-cell membrane interactions and its influence on intracellular trafficking of nanoparticles. *Biomaterials* **2008**, *29*, 4244–4252.

(42) Gallucci, S.; Lolkema, M.; Matzinger, P. Natural adjuvants: Endogenous activators of dendritic cells. *Nat. Med.* **1999**, *5* (11), 1249–55.

(43) Seong, S. Y.; Matzinger, P. Hydrophobicity: an ancient damage-associated molecular pattern that initiates innate immune responses. *Nat. Rev. Immunol.* **2004**, *4* (6), 469–78.